Vacuum UV photodesorption of organics in the interstellar medium: an experimental study of formic acid HCOOH and methyl formate HCOOCH 3 -containing ices

Mathieu Bertin, Romain Basalgète, Antonio Ocaña, Géraldine Féraud, Claire Romanzin, Laurent Philippe, Xavier Michaut, Jean-Hugues Fillion

Journal Name

ARTICLE TYPE

Cite this: DOI: 00.0000/xxxxxxxxxx

Vacuum UV photodesorption of organics in the interstellar medium: an experimental study of formic acid HCOOH and methyl formate $HCOOCH_3$-containing ices

Mathieu Bertin,*[a] Romain Basalgète,[a] Antonio J. Ocaña,[a] Géraldine Féraud,[a] Claire Romanzin,[b] Laurent Philippe,[a] Xavier Michaut,[a] and Jean-Hugues Fillion,[a]

Received Date
Accepted Date

DOI: 00.0000/xxxxxxxxxx

Being a potential process that could explain gas phase abundances of so-called Complex Organic Molecules (COMs) in the cold interstellar medium (ISM), the UV photon-induced desorption from organics-containing molecular ices has been experimentally studied. In this work, we focused on the observation of the photodesorbed products and the measurement of the associated photodesorption yields from pure and mixed molecular ices, each containing organic molecules whose detection has been achieved in the gas phase of the cold ISM, namely formic acid HCOOH and methyl formate $HCOOCH_3$. Each molecule, in pure ice or in ice mixed with CO or water, was irradiated at 15 K with monochromatic vacuum UV photons in the 7-14 eV range using synchrotron radiation from the SOLEIL synchrotron facility, DESIRS beamline. Photodesorption yields of the intact molecules and of the photoproducts were derived as a function of the incident photon energy. Experiments have revealed that the desorbing species match the photodissociation pattern of each isolated molecule, with little influence of the kind of ice (pure or mixed in CO or H_2O-rich environment). For both species, the photodesorption of the intact organics is found negligible in our experimental conditions, resulting in yields typically below 10^{-5} ejected molecules per incident photon. The results obtained on HCOOH and $HCOOCH_3$-containing ices are similar to what has already been found for methanol-containing ices, but contrast with the case of another complex molecule, CH_3CN, photodesorption of which has been recently studied. Such experimental results may be linked to the observation of COMs in protoplanetary disks, in which CH_3CN is commonly observed whereas HCOOH or methanol are detected only in some sources, $HCOOCH_3$ not being detected at all.

1 Introduction

This last decade, the presence of small organic molecules – usually referred to as Complex Organic Molecules (COMs) – was evidenced in the gas phase of the coldest regions of the interstellar medium (ISM). Among COMs, gaseous methyl formate $HCOOCH_3$ is detected in several prestellar cores[1–3], while gaseous formic acid HCOOH is observed in prestellar cores[3,4], in low UV flux photon-dominated regions PDR[5] and in protoplanetary disks[6]. In any case, the observations of such COMs in these cold regions (T $\sim$ 10-30 K) is still puzzling, since both their formation and their detection in the gas phase have to be explained without available thermal energy.

The exact formation mechanisms of these species are still unclear. Gas phase chemical routes are possible at low temperature, but rather unlikely – they involve the presence of gaseous ethanol for the formation of HCOOH, or a several step chemical process initiated from methanol for the formation of $HCOOCH_3$[7–9]. Other potential origins of these molecules may involve the solid phase chemistry in the icy mantles coating the interstellar dust grains in the cold regions. For instance, the formation of HCOOH and $HCOOCH_3$ can proceed through hydrogenation and hydroxylation of the CO-rich phase of the ice mantle[10,11], or be triggered by cosmic rays (CR)-induced or UV photon-induced chemistry in pure methanol ices[12] or more realistic H_2O:CO and H_2O:CH_3OH icy mixtures[13].

In any case, due to the very low temperatures of the media in which they are detected, the presence of HCOOH and $HCOOCH_3$ in the gas phase has to involve a non-thermal mechanism which either counterbalance their depletion on the dust grains if they are formed in the gas, or eject the molecules from the icy mantles if they are formed in the solid phase. Several non-thermal desorption mechanisms may fulfill this role, such as the sputtering of the ice mantle by shocks between grains, the CR-induced sputtering of the icy mantles, the exothermicity of the formation reaction

[a] Sorbonne Université, Observatoire de Paris, PSL university, CNRS, LERMA, F-75005, Paris, France E-mail: mathieu.bertin@sorbonne-universite.fr
[b] Univ. Paris-Saclay, CNRS UMR 8000, ICP, F-91405, Orsay, France.

on the grain surface which releases a part of the product in the gas phase – a process usually referred to as chemical desorption –, and the desorption induced by VUV or X-ray photons absorption in the ice mantle, also called VUV or X-ray photodesorption. Therefore, proper modelling of the chemistry of COMs in the cold ISM requires to quantitatively constrain both the chemical formation of organics, and their non-thermal desorption processes[14]. This in return implies it is necessary to perform quantitative studies that provide desorption yields for these organics in physical-chemical conditions relevant to the cold ISM. However, to date, very little experimental data dealing with non-thermal desorption efficiencies of COMs exist, with the notable exception of the methanol molecule. VUV photodesorption[15,16], X-ray photodesorption[17,18] and CR sputtering[19,20] yields of methanol have been experimentally measured from methanol-containing ices, which concluded on the preponderant role played by CR in dense cores, compared to the secondary UV photons. Chemical desorption of methanol has also been experimentally studied, although only upper limits could be proposed because of the lack of experimental evidence[21]. The non-thermal desorption of the other COMs is left mainly unexplored, and usually the results obtained in the case of methanol are used as representative of a general trend followed by all the other organics. However, a recent study of the UV photodesorption of acetonitrile CH_3CN has revealed a different behaviour as compared to methanol, hinting that experimental results obtained from methanol-containing ice cannot *a priori* be extrapolated to the case of any other organics for the UV-induced processes[22]. In the case of both HCOOH and $HCOOCH_3$, there exists to our knowledge no experimental constrain for non-thermal desorption in general, and for UV photodesorption in particular.

Here, we present an experimental study dealing with the UV photodesorption from HCOOH and $HCOOCH_3$ containing ices, with the double aim of shedding light on the photodesorption mechanisms and properties, and of providing photodesorption yields for any desorbing species from these ices applicable to different regions of the ISM. Each molecule is studied as a pure ice, and in physisorbed binary mixtures organics:CO and organics:H_2O, believed to be more representative of the composition of the outer layers of the interstellar ices on either sides of the CO freeze-out region[23,24]. The tunable output of the SOLEIL synchrotron facility, DESIRS beamline, is used to irradiate the ices at several energies in the 7 - 14 eV range, allowing to derive photon energy-resolved photodesorption yields of each desorbing species, and finally astrophysical desorption yields which take into account the spectral structure of the UV fields in different regions of the interstellar medium. The obtained values are then discussed in regards of observations of these COMs in the cold ISM, and of already-characterized photodesorption from other COM-containing ices, such as methanol and acetonitrile.

2 Experimental methods

The studies are realized in the UltraHigh Vacuum (UHV, base pressure $\sim 2\times10^{-10}$ Torr) setup SPICES (Surface Processes & ICES) installed at the LERMA (Sorbonne University, Paris). The molecular ices are grown on a polycrystalline High Conductivity, Oxygen-Free (OFHC) copper substrate, mounted on the tip of the rotatable cold head of a closed-cycle helium cryostat. Its temperature can be varied from 13 K to 300 K, with an absolute precision better than 0.5 K, and a relative stability within 0.1 K, even during UV irradiation. The ices are prepared in situ by exposing the cold substrate to a partial pressure of the desired molecules, through a dosing tube positioned a few millimeters away in front of the surface - thus allowing to deposit relatively thick ices ($\sim$ 100 monolayers ML) with a limited increase of the base pressure in the chamber (typically only a few 10^{-9} Torr during the ice growth). A calibration method based on the use of the Temperature Programmed Desorption (TPD) technique allows preparation of ice of chosen thickness, expressed in monolayers ML – one ML being equivalent to the surface density of a saturated molecular layer on the surface, roughly 10^{15} molecules/cm^2 – with a relative precision of about 10 % (see e.g.[25] or[26]).

In this study, ices of formic acid HCOOH and methyl formate $HCOOCH_3$ were prepared, pure and mixed with either CO or H_2O. Pure liquids of HCOOH (Sigma-Aldrich, >98 % purity), $HCOOCH_3$ (Sigma-Aldrich, 99 % purity) and H_2O (Fluka, liquid chromatography standard) were further purified using freeze-pump-thaw cycles. CO (Air Liquide, >99.9 % purity) was used with no further purification. Each species' purity was checked in situ using mass spectrometry. Pure organic ices and ices mixed with CO were grown at 15 K, while ices containing H_2O were prepared at 90 K, to ensure the resulting water ice is in its compact amorphous phase (also referred to as c-ASW, standing for compact Amorphous Solid Water), and then cooled down to 15 K for the irradiation experiments. Icy mixtures were grown by first preparing a few mbar of gaseous mixture of the two constituents, composition of which is controlled by two sets of capacitive pressure gauge in the gas introduction system. The gaseous mixture was then introduced in the UHV chamber and deposited onto the cold copper substrate. The resulting ice composition was first calibrated using TPD technique before the experiments, and further checked by systematically performing TPD on each sample after irradiation.

To study the photodesorption from the ices, the Vacuum UV (VUV) output of the DESIRS beamline from the synchrotron SOLEIL facility (St Aubin, France) was used. The SPICES setup was directly connected to the end of the beamline, without any window, thus preventing cut-off at high photon energies. The DESIRS beamline provides VUV photons, energy of which is tunable by means of an undulator, coupled to a gas filter to suppress high energy harmonics[27]. In these experiments, typical photon energy range of 7 - 14 eV was used. Prior to its introduction in the chamber, the photon beam is reflected onto a grating. In the presented results, the 0 diffraction order was used, resulting in a higher flux but lower resolution mode. The photon flux is measured using a calibrated photodiode, and varies between 6×10^{14} photons/s at 7 eV and 6×10^{13} photons/s at 14 eV. The energy resolution in this mode is of $\sim$ 1 eV.

The VUV beam is sent with a 47° incidence angle on the samples, and irradiates a surface of $\sim$ 1 cm^2. During irradiation, the photodesorption of neutrals is monitored as a function of the photon energy by means of a Quadripolar Mass Spectrometer (QMS) using electron-impact ionization at 70 eV. The photon energy scan

is made as follows: the ice is irradiated at a fixed energy using the 0 order of the grating during about 30 s, the beam is shut and the energy changed to the next desired value. During each irradiation step, the desorbing species are probed using the mass channel corresponding to their intact cation. An example of the acquired data is given in the figure 1 in the case of photodesorption from pure formic acid at 15 K. At each irradiation energy, the amplitude of the mass signals – corrected from the background – is defined as the desorption signal, and is converted to photodesorption yields **using the following protocol. The energy resolved desorption yield $\Gamma_X(E)$ of a given species X is derived from the desorption signal $I_{X^+}(E)$ of the cation X^+, corrected from the photon flux $\Phi(E)$ at the photon energy E following:**

$$\Gamma_X(E) = A_X \frac{I_{X^+}(E)}{\Phi(E)}$$

where A_X is a calibration factor for the species X. The factors are determined experimentally by first recording a calibration photodesorption spectrum of CO from a 50 ML CO ice, and comparing it to the already well-constrained CO photodesorption yields in the literature[28]. From this, the calibration factor A_{CO} for CO molecule is determined. All the other calibration factors are then extrapolated from A_{CO} considering different electron-impact ionization efficiencies in the mass spectrometer and different sensitivity of the mass spectrometer depending on the mass of X, also referred to as the apparatus function AF:

$$A_X = A_{CO} \frac{AF(X)}{AF(CO)} \frac{\sigma(CO^+/CO)}{\sigma(X^+/X)}$$

with $\sigma(X^+/X)$ being the partial electron-impact ionization cross section at 70 eV of X giving X^+ and $AF(X)$ the apparatus function of our spectrometer determined by comparing mass spectra of known species to reference data from the NIST chemical webbook[29]. Values from the literature were used for the ionization of CH_3, OH, H_2O, CO, H_2CO, O_2, CO_2, HCOOH and $HCOOCH_3$[30–35]. Values for HCO and H_3CO were not available, and the ionization cross section for H_2CO were used for these two species. Finally, since the dissociative ionization of heavier species may participate to the signal of X^+, each desorption signals were corrected from the dissociation of the higher mass signals by taking into account the dissociation branching ratio at 70 eV and the mass-dependent apparatus functions.

Independently from the signal-to-noise ratio, this calibration procedure comes with a systematic uncertainty which comprises uncertainties on (i) the published values of the ionization cross sections, (ii) on the CO molecule desorption yields, and (iii) on the apparatus function determination, but also uncertainties associated with the method itself, which in particular neglects the effects of different kinetic energies and spatial dispersion the desorbing molecules may have as compared to the CO molecules. Overall, we estimate this systematic uncertainty to be in the order of 50 % of the derived photodesorption yields.

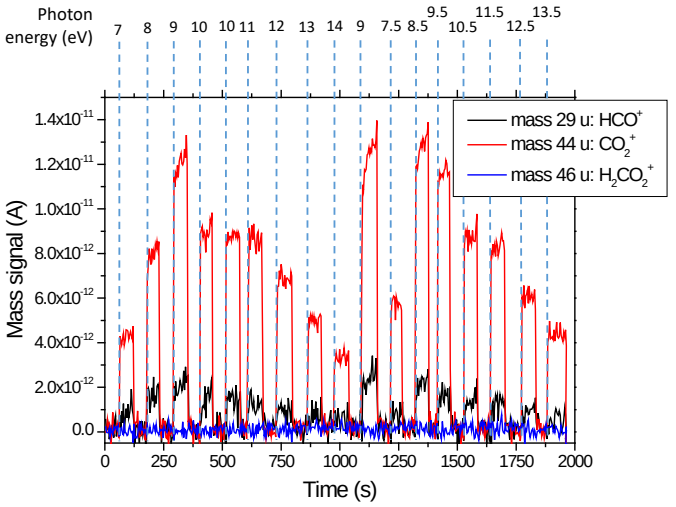

Fig. 1 Mass signals of several desorbing species during irradiation at several energies of pure 60 ML of formic acid at 15 K. Vertical lines indicate the moment where the VUV photons are introduced in the experiment. The mass signals are corrected from the continuous background signal due to the residual vacuum in the chamber.

It should be noted here that only desorption of neutrals has been measured, and searched for, in this study. However, we do not expect the positive ion photodesorption to be an important desorption pathway in this energy domain. Indeed, it is suggested in past studies, e.g. by Philippe et al.[36] in the case of a CO ice, that the threshold for ion desorption exceeds 15 eV, and proceeds through the excitation of high-energy lying autoionized Rydberg states, well above the ionization potential – and also out of our probed energy range. Furthermore, the ion desorption yield becomes important only at even higher energies (> 25 eV) when excited state of the ion can be populated. Accordingly, previous attempts to measure photodesorption of ions in the 7 - 14 eV range from more simple ices (pure H_2O, CO and CO_2) were not successful in our case. We expect that ion desorption from HCOOH and $HCOOCH_3$ is also very weak in our energy range, and probably negligible as compared to neutral desorption.

Finally, the ices are probed during and after irradiation by two complementary techniques: Reflection Absorption InfraRed Spectroscopy (RAIRS), performed by means of a Brucker vec22 Fourier-transform infrared spectrometer used with a resolution of 1 cm^{-1}, coupled to the main chamber by in-vacuum optics and KBr windows, and the TPD technique, which consists in applying a constant heating ramp to the sample, and monitoring the desorbed species as a function of the sample's temperature. Both methods are used in order to identify any photochemistry which may have occured during the irradiation.

3 Results and discussion

3.1 Photon-induced modifications in the HCOOH and $HCOOCH_3$-containing ices probed by infrared spectroscopy

Fourier Transform - Reflection Absorption InfraRed Spectroscopy (FT-RAIRS) was systematically performed on the studied ices, after their growth and their irradiation at several energies in the 7-14 eV range. The obtained infrared spectra are shown in Fig. 2, on HCOOH-containing ices and $HCOOCH_3$-containing ices, after deposition, and after irradiation at 15 K. Each ice has been irradiated by the equivalent of a photon energy scan in the 7-14 eV energy range, representing a total photon fluence of about 10^{17} cm^{-2}. The IR spectra of the pure organics in the solid phase were attributed following works by Bertin et al.[37] for $HCOOCH_3$ and Bennett et al.[38] for HCOOH. IR spectra of mixed ices consist mainly in the superimposition of the organics-related vibrations with the most intense vibrations of solid water ice (broad OH-stretching features around 3400 cm^{-1} and libration mode features around 850 cm^{-1}, the bending mode overlapping with the C=O stretching vibration of the organics) or the solid CO vibration (sharp peak at $\sim$ 2140 cm^{-1}). Slight shifts in the band positions or modifications in the width of the vibrational features are observed depending on the composition of the ice; an effect being associated with different intermolecular interactions which modify the involved bond-strengths. After VUV irradiation, the only clearly observed modification of the IR spectra is the appearance of two bands at 2345 and 2140 cm^{-1} which are associated with condensed CO_2 and CO respectively, and a general slight decrease of the organics-related vibrational signatures. In the case of organics mixed with CO, a very small increase in the intensity of the CO band is observed. Our experiments do not highlight the appearance of more complex molecules after irradiation, – that would be observed via the appearance of new vibrational features –, indicating that either more complex products are formed in too small quantity for us to detect, or that their vibrational signatures overlap with those of the non-irradiated ices. Except for the CO and CO_2 formation in the solids, the pure and mixed ices remain mostly intact after the irradiation in our flux and fluence conditions, as shown by their IR spectra which are only weakly altered, and still dominated by the organics and either water or CO vibrational features.

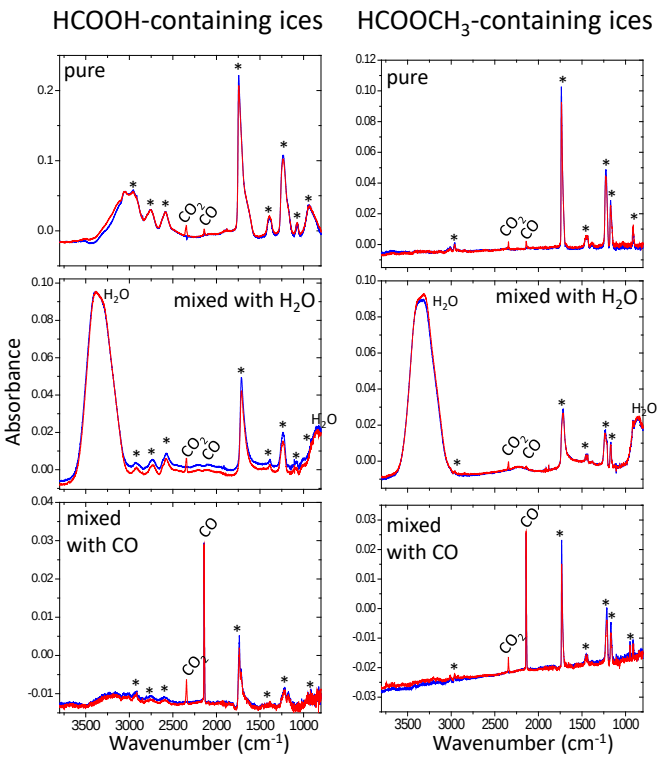

Fig. 2 IR spectra of HCOOH (left) and $HCOOCH_3$ (right)-containing ices after deposition (blue spectra) and after irradiation (red spectra) at 15 K. Each organics has been deposited in 60 ML of pure ices (upper line), in condensed mixture organics:H_2O (1:10 for HCOOH:H_2O and 1:3 for $HCOOCH_3$:H_2O – central line), and in mixture organics:CO (1:10 – lower line). Positions of the vibrational feature associated with each organic molecule are indicated with *. Each ice was irradiated with varying incident photon energy between 7 and 14 eV with a total fluence of about 10^{17} cm^{-2}.

3.2 Desorption from pure HCOOH and $HCOOCH_3$ ices

Experiments realized on pure ices of formic acid and methyl formate kept at 15 K have revealed the desorption of a collection of neutral species. The associated photodesorption yields as a function of the photon energy are presented in Fig. 3 and Fig. 4. In these figures, the mass channels 18 u, 28 u, and 44 u were attributed to the desorption of H_2O, CO and CO_2 respectively, desorption of which are observed both from HCOOH and $HCOOCH_3$. The origin of the mass 32 u signal measured in the case of photodesorption from $HCOOCH_3$ (Fig. 4) has been mainly attributed to O_2 desorption. Mass 32 u could also correspond to the CH_3OH^+ ion resulting from the ionization of some desorbing methanol CH_3OH or dissociative ionization of $HCOOCH_3$ in the QMS. The latter has been ruled out since no $HCOOCH_3^+$ ion was detected during the experiments. Methanol dissociative ionization in the QMS is also expected to produce an important signal on the 31 u mass channel – actually bigger than the 32 u signal – associated with the CH_3O^+ ion[29]. In our case, we indeed detect a small signal on the mass channel 31 u, but almost three times weaker than the signal on the 32 u channel, thus ruling out the fact that 32 u solely corresponds to methanol. Moreover, if one considers that the signal at 32 u is only O_2, then the correction of its dissociative ionization into the QMS brings the level of a small signal detected on the mass 16 u channel exactly to 0 (within error bars, and after correction from the water dissociative ionization). This further motivated our attribution of mass 32 u as O_2 and mass 31 u as the H_3CO radical ionization, even if the desorption of a very small quantity of methanol, participating as a small amount to these two mass signals, cannot be totally ruled out. Finally, the signals at 15, 29 and 30 u were attributed to the desorption of radicals CH_3, HCO, and H_2CO respectively.

In the case of condensed HCOOH, the desorption yields of each species follow the same energy dependence, depicting a constant

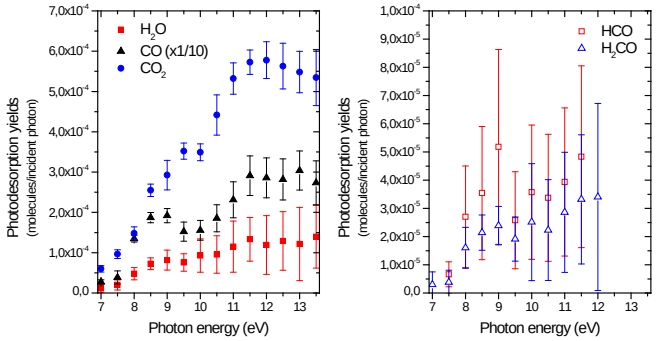

Fig. 3 Photodesorption yields of all the detected neutral species from 60 ML of pure ice of formic acid HCOOH at 15 K. Yields for the mass channel 29 and 30 u (associated with desorption of HCO and H_2CO respectively) could not be confidently isolated from the noise for photon energies above 12 eV, and are thus not shown. For clarity, the photodesorption yield of CO was divided by 10.

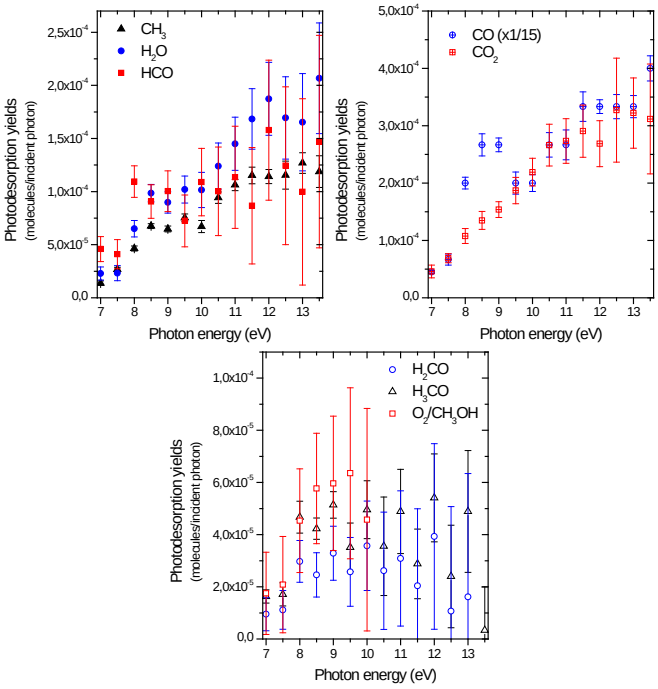

Fig. 4 Photodesorption yields of all the detected neutral species from 60 ML of pure ice of methyl formate $HCOOCH_3$ at 15 K. Yields for the mass channel 32 u (associated with desorption of mainly O_2, and probably some CH_3OH) could not be isolated from the noise for photon energies above 10 eV, and are thus not shown. For clarity, the photodesorption yield of CO was divided by 15.

increase over the whole energy range, with a small local depth at around 10 eV. We thus expect this structure to be representative of the VUV absorption spectrum of solid HCOOH, even if, such data being not available in the litterature, a direct comparison was not possible. The same observation can be made from the desorption yields from solid $HCOOCH_3$, for which most of the energy-dependences are identical (within error bars), but VUV absorption spectrum of which is not available to our knowledge. However, a notable exception is the CO photodesorption yields, which presents a clear local maximum at 8.5±0.5 eV. This structure can be associated with the solid CO absorption feature related to the $A(^1\Pi)$-$X(^1\Sigma^+)$ transition, which presents a structured vibronic band in this energy range[39,40] strongly coupled to the desorption[28]. Indeed, during irradiation, some of the formed CO can remain in the condensed phase, in return available to absorb another photon and desorb. This phenomenon, due to the accumulation of photoproduced CO in the solid, has already been observed in the case of pure CO_2 ices[41], and infrared spectroscopy has confirmed the formation and accumulation of CO in the irradiated $HCOOCH_3$ ice after irradiation (see the electronic supplementary information.†).

Pure ices of both HCOOH and $HCOOCH_3$ behave similarly under VUV irradiation. Probably the most striking finding of these experiments is that no photodesorption of the intact molecule could be measured. For both species, the photodesorption is dominated by the desorption of the CO molecule, followed by the desorption of CO_2 and H_2O. O_2, CH_3 and H_3CO could only be detected from pure $HCOOCH_3$, while HCO and H_2CO were detected from both HCOOH and $HCOOCH_3$ ices. In fact, those species match the direct photodissiociation pattern of both HCOOH and $HCOOCH_3$ as studied in the gas phase. Photodissociation of gas phase HCOOH in the UV and VUV range results in the following fragmentations[42–46]:

$$\begin{aligned} HCOOH + h\nu \longrightarrow\ & CO + H_2O && (1)\\ & CO + H + OH && (2)\\ & CO_2 + H_2 && (3)\\ & HCOO + H && (4)\\ & HCO + OH && (5) \end{aligned}$$

Except for the channel (4), each of these dissociation pathways can explain the detected photodesorbed species. H and H_2 cannot be confidently detected by our QMS, and OH may actually photodesorb, but could not be separated from background noise after correction of H_2O dissociative ionization on the 17 u mass signal. Desorption of some H_2CO is also detected, but is not explained by photodissociation of the HCOOH as known from gas phase experiments. This could be due either to a dissociation pathway specific to the condensed phase, or to the result of subsequent chemistry in the ice, e.g. triggered by hydrogen atoms released from channel (4), leading to the H_2CO formation and desorption.

Gas phase $HCOOCH_3$ photodissociation in the UV has also been studied, e.g. by Schwell *et al.*[45], Lee[47] and Nakamura *et al.*[48]. The main identified dissociations channels are:

$$\begin{aligned} HCOOCH_3 + h\nu \longrightarrow\ & CH_3O + CO + H && (6)\\ & CH_3O + HCO && (7)\\ & CH_3OH + CO && (8)\\ & CH_3 + CO_2 + H && (9) \end{aligned}$$

If one considers similar fragmentation patterns in the solid phase, detected desorbing CO, CO_2, CH_3, HCO and H_3CO from pure solid $HCOOCH_3$ can all be attributed to direct photodissociation of the condensed methyl formate molecules. However, gas phase studies do not highlight H_2O, O_2 or H_2CO as results of photodissociation of methyl formate. Similarly as the case of H_2CO from HCOOH, those species may originate from different dissociation pathways or from photochemistry in the solid $HCOOCH_3$ coupled to desorption.

3.3 desorption from HCOOH and $HCOOCH_3$ in H_2O- and CO-rich ices

In order to estimate the role played by the molecular environment on the photodesorption, model ices of HCOOH and $HCOOCH_3$ embedded in a CO or H_2O-rich ice were studied. For each organics, four kind of mixed ices were investigated: icy mixture of CO:organics and H_2O:organics, in which either CO or H_2O were in excess, or layered ices consisting of 1 ML of organics deposited onto a pure CO or pure compact amorphous H_2O ice. Fig. 5 presents an overview of the desorbing species, together with their photodesorption yields, for an irradiation at the photon energy of 10 ± 0.5 eV. As in the case of pure ices, no signal associated with the desorption of the intact HCOOH or $HCOOCH_3$ molecule could be detected. In these cases, only an upper limit, defined as the noise amplitude on the mass channel, can be derived from our data. For each ice, all the desorbing species are identical to the case of pure organics ices, at the notable exception of OH and O_2 desorptions which are detected from HCOOH-containing ices only when formic acid is coadsorbed with H_2O. This indicates the weak role played, in our flux and fluence conditions, by the photochemistry involving both the organics and the surrounding water or CO, or at least that potentiel photochemistry is not correlated to the desorption phenomenon. This is further corroborated by the fact that most of the desorbing species (HCO, H_2CO and to some extent CO_2 for HCOOH; CH_3, HCO, H_2CO, H_3CO, O_2 and CO_2 for $HCOOCH_3$) present very similar photodesorption yields, most of the time identical within error bar for each system, pure or mixed. This stresses that these species most likely originate from the dissociation of the organics alone, and that that their desorption does not depend on the local molecular environment.

CO desorption is slightly enhanced when the organics are codeposited with CO molecules - especially in the case of HCOOH-containing ices. Indeed, CO weakly absorbs, and photodesorbs, in the 9.5 - 10.5 eV region[28], and thus some of the detected CO from mixed ices originates from the excitation and desorption of the co-deposited CO molecules. The H_2O photodesorption yields are also found poorly dependent on the ice, and almost not varying when the organics are mixed with water. This is suprising at first since some codeposited H_2O is expected to photodesorb when irradiated, and thus should, together with the dissociation of the organics, contribute to the total H_2O desorption yield. VUV photodesorption yield of H_2O from pure water ices at $\sim$10 eV are experimentally estimated between 5×10^{-4} and 1×10^{-3} molecules/photon, the latter value being derived from an amorphous porous ice and not a compact one[49–51]. Here, H_2O desorption yields are found at best more than two times lower, even from ices mixed with water. An explanation would be that coadsorption with organics prevents the desorption from the condensed water. Indeed, Fillion *et al.*[51] propose that the water photodesorption process from pure water ice, under our flux and fluence conditions, are due to a large extent to the photochemistry at the ice surface, reforming H_2O molecules from H and OH radicals, which then desorb. Adjunction of organics in the vicinity may perturbate this chemistry and hinder the water desorption by recombination, leaving mainly the organics fragmentation as a source of gas phase H_2O. OH and O_2 desorption are observed during irradiation of HCOOH:H_2O mixed ices, but are not detected from pure HCOOH ice or in HCOOH:CO mixtures. These desorptions may originate from the desorption from the solid water itself, since the measured yields are comparable to the O_2 and OH photodesorption yields from pure water ice[50–52]. However, O_2 desorption is not modified in the case of $HCOOCH_3$ mixed with water, and no OH signal could be measured for these systems. However, contrary to the case of methyl formate, OH is expected to be formed via the dissociation of HCOOH, even if its desorption from pure formic acid could not be detected. Since OH is also expected to be produced from water itself, the irradiation of the mixture HCOOH:H_2O may increase its production to the point where it exceeds our detection limit, explaining thus its observation in this case. The origin of O_2 desorption from HCOOH:H_2O mixed ice is still unclear, but it may also be linked to the increased production of OH radicals, as compared to the other systems. Indeed, OH radicals are at the origin of the O_2 production in irradiated water ice as demonstrated by UV photon or electron irradiation experiments.[51,53] Such process in our case may trigger some surface chemistry releasing some O_2 in the gas phase. Different HCOOH dissociation branching ratio at the surface of the water ice, leading to O_2 formation, cannot not however be ruled-out. Finally, desorption of HCO is not detected anymore when $HCOOCH_3$ is mixed in a H_2O-rich environment. HCO is believed to originate from the photodissociation of methyl formate also leading to some H_3CO production, desorption of which is not affected by the coadsorption with water molecules. The absence of HCO desorption is still unclear, but may be associated to some chemistry between the radical HCO and H_2O molecules or other photoproducts. A similar effect is also observed in the HCOOH:H_2O ices, for which the HCO desorption is also found below the detection limit. Our studies do not bring evidence, however, of this chemistry, which may lead e.g. to some CO and CO_2 production, as it cannot be disentangled from the much higher quantities already detected directly from the dissociation of the organics.

Photon energy-dependent photodesorption yields from the mixed ices were also measured. Some example of photodesorption yields from mixed ices are shown in Fig. 6 and 7. Except for the CO desorption from CO-containing ices, the global shape of the desorption spectra reflect the ones of the pure HCOOH or $HCOOCH_3$. There again, the strong similarities between the pure and the mixed organics suggests that most of the observed desorption is due to the organics absorption and subsequent dissociation, and that the matrix plays here a minor role. The low energy

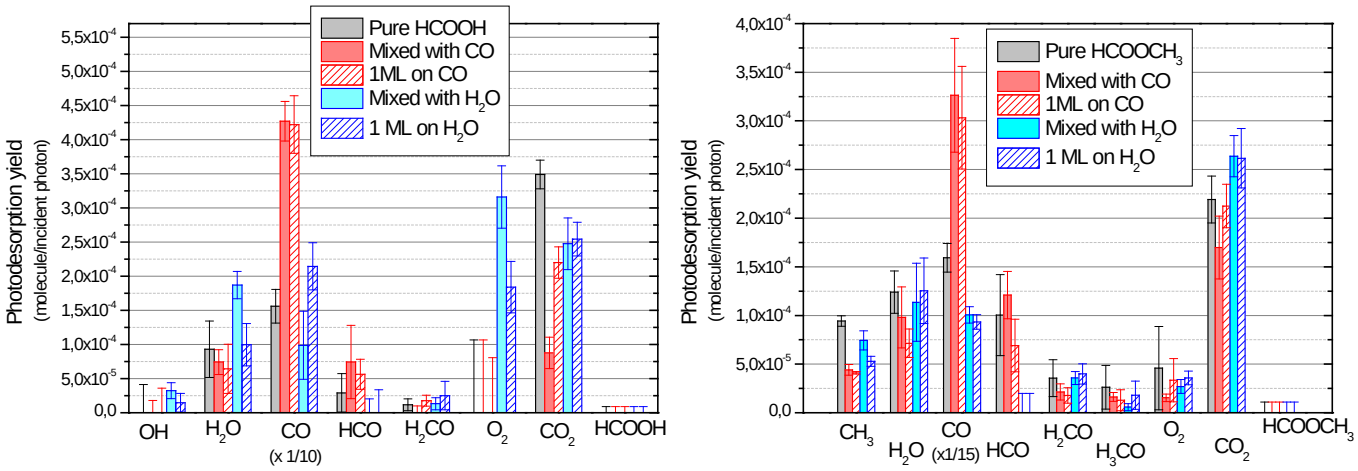

Fig. 5 Photodesorption yields of neutral species from HCOOH and $HCOOCH_3$-containing ices at 15 K, during irradiation with 10±0.5 eV photons and a flux of 2.3×10^{14} photons/s. Left: photodesorption from 60 ML of pure HCOOH, HCOOH mixed in 60 ML of CO (1:10), HCOOH mixed in 60 ML of H_2O (1:10), 1 ML HCOOH on top of 30 ML of CO, and 1 ML HCOOH on top of 30 ML of H_2O. Right : photodesorption from 60 ML of pure $HCOOCH_3$, $HCOOCH_3$ mixed in 60 ML of CO (1:10), $HCOOCH_3$ mixed in 60 ML of H_2O (1:3), 1 ML $HCOOCH_3$ on top of 30 ML of CO, and 1 ML $HCOOCH_3$ on top of 30 ML of H_2O. The photodesorption yields of CO were artificially divided by 10 (left panel) and 15 (right panel) for clarity.

resolution employed here, the error bars and the broadness of the spectra prevent however to totally rule out any contribution of the H_2O or CO absorption in the photodesorption yields of water and CO-containing ice. It is clear however that those contributions should be minimal.

3.4 Discussions and astrophysical implications

Our experiments have revealed that the UV photodesorption from HCOOH and $HCOOCH_3$-containing ices is dominated by the photodissociation of the organics and the subsequent desorption of the photofragments in the gas phase. Whatever is the composition of the studied ices, the desorption of the intact organics could not be detected. Only an upper limit for the desorption yields can be derived from our measurements. The experimental photodesorption yields as a function of the photon energy can be used to calculate averaged photodesorption yields for each detected species, taking into account the spectral structure of the UV fields in the ISM. Table 1 presents these astronomical photodesorption yields for several interstellar UV spectra, that may be of use in different regions of the ISM, such as the InterStellar Radiation Field ISRF for PDR-like border regions[54], secondary photons from cosmic-ray ionization for dense cores[55] and inner regions of disks[56]. The two latter are mostly dominated by a strong H Ly-α component at 10.2 eV, and they both lead to very similar values – equal within our error bars – for the averaged photodesorption yields. As discussed previously, we found that the VUV photodesorption from the COMs does not strongly depend on the presence of either CO or H_2O molecules in the ices (an exception however is the case of HCO, photodesorption of which being hindered in the case of mixed water:HCOOH and water:$HCOOCH_3$ ices). Accordingly, we took the photodesorption spectra from pure ices of COMs to derive the yields of Table 1, which we assume to be applicable in the case of any mixed ices containing each of the COMs and CO or H_2O.

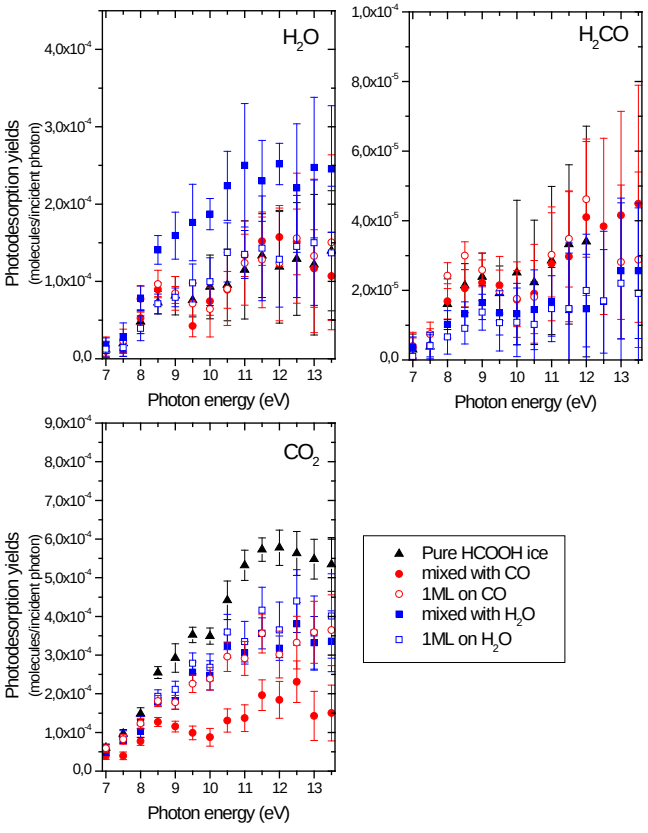

Fig. 6 Photodesorption yields of some neutral species (H_2O, H_2CO and CO_2) from 60 ML formic acid-containing ices at 15 K : pure ice of HCOOH, 1 ML of HCOOH onto pure ices of CO and H_2O, HCOOH:CO and HCOOH:H_2O mixed ice in proportion 1:10.

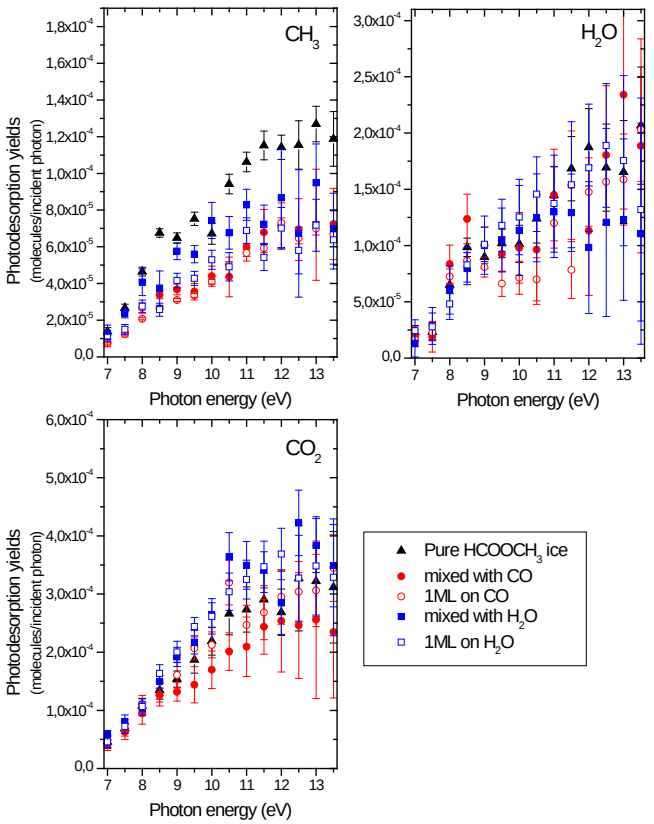

Fig. 7 Photodesorption yields of some neutral species (CH_3, H_2O and CO_2) from methyl formate-containing ices at 15 K : pure ice of $HCOOCH_3$, 1 ML of $HCOOCH_3$ onto pure ices of CO and H_2O, $HCOOCH_3$:CO and $HCOOCH_3$:H_2O mixed ice in proportion 1:10 and 1:3 respectively.

The fact that the desorption yields of the intact molecules are found below of our detection limits, independently from the ice (pure, mixed with H_2O or CO), is an important and interesting finding. First, it points out that the photodissociation of the molecules is a more efficient decay pathway subsequent to the photon absorption of a photon by the organics, thus competing with the desorption which becomes comparatively negligible. Potential photochemistry in the ice does not participate to the reformation and desorption of the initial organics, as it is for instance the case of H_2O desorption from pure water ices[51]. Second, it also points out that the surrounding molecules, in our case CO and H_2O, do not promote the desorption of the organics, as it is the case for more simple coadsorbed molecules. Indeed, some studies on UV photodesorption from simple molecules (N_2, CH_4, CO, CO_2) or rare gas atoms adsorbed on a CO or H_2O-rich ice have shown that the absorption of a photon by the dominant species, i.e. CO or H_2O, could trigger the desorption of the coadsorbed species. This indirect desorption process is known to proceed either via a kick-out mechanism in the case of species coadsorbed with water – during which an hydrogen atom from H_2O photodissociation collides with a surface molecule or atom, giving it enough momentum to overcome the adsorption barrier and desorb[57] – or via another kind of energy transfer, which remains to be clarified, in the case of CO[58,59]. Such indirect processes may have a strong influence when it comes to modelize UV photodesorption from interstellar ices since the photodesortion yields of such simple species actually depend on the ice composition. Obviously, in the case of HCOOH and $HCOOCH_3$, such indirect desorption, promoted by the photon absorption by the main constituents CO or H_2O, is either not operative, or too weak to produce enough gas phase organics for us to detect. There can be several explanations for this. One of those could be that HCOOH and $HCOOCH_3$ present many internal degrees of freedom as compared to simple molecules such as N_2, and thus any external energy brought by the matrix to the molecule can be dissipated into internal energy, lowering the amount of energy left in the translation for the molecules to desorb. Another could be due to the higher strength of intermolecular interactions in the solids when organics are involved, via hydrogen bounding implying the hydroxyl –OH and carboxyl –C=O groups for instance, which are not encountered in the case of simpler species for which only weaker van der Waals interactions are at play.

To many respects, the UV photodesorption from HCOOH and $HCOOCH_3$-containing ices is very similar to the one from methanol-containing ice. Indeed, UV photodesorption yields of CH_3OH is close to our detection limit from pure methanol ices, and is not detected in the case of mixed ices methanol:CO (yields below 3×10^{-6} molecules/photon). Instead, the photodesorption from methanol is dominated by the desorption of its photodissociation products[15,16]. HCOOH and $HCOOCH_3$ seem to follow the same tendencies, e.g. a weak photodesorption of the intact molecules – in these cases not even detected –, not promoted by the molecular environment, and a desorption mostly reflecting the photodissociation of the species. This does not, however, mean that it is a general trend for all the organic species that can be encountered in the interstellar ices. Indeed, recent

Table 1 Astronomical photodesorption yields ($\times 10^{-5}$ desorbed molecule per incident photon) derived from the experimental photon-energy resolved yields of HCOOH and $HCOOCH_3$-containing ices and UV spectra relevant to PDR and dense cores or inner regions of disks. Associated uncertainties take into account signal-over-noise ratio and the systematic relative uncertainty of ∼50 % related to the quantification method

Photodesorbed species	ISRF[a]	Dense clouds[b] and disks[c]
From HCOOH-containing ices		
HCOOH	< 0.5	< 0.5
CO_2	14 ± 7	36 ± 18
H_2CO	0.7 ± 0.4	2.1 ± 1.1
HCO[d]	1.0 ± 0.5	3.1 ± 1.6
CO	73 ± 36	170 ± 90
H_2O	3.4 ± 1.7	8.7 ± 4.4
From $HCOOCH_3$-containing ices		
$HCOOCH_3$	< 1	< 1
CO_2	7.9 ± 4	22 ± 11
H_3CO	1.0 ± 0.5	3.0 ± 1.5
H_2CO	1.6 ± 0.8	4.1 ± 2.1
O_2	1.0 ± 0.7	1.2 ± 0.9
HCO[d]	3.8 ± 1.9	10 ± 5
CO	140 ± 70	340 ± 170
H_2O	4.3 ± 2.2	11 ± 6
CH_3	3.1 ± 1.6	7.5 ± 3.8

Using UV fields from [a] Mathis *et al.* [54], [b] Gredel *et al.* [55] and [c] France *et al.* [56].
[d] when mixed in H_2O-rich ices, the photodesorption yields of HCO is hindered and drop below our detection limit ($< 2 \times 10^{-5}$).

studies on the photodesorption of acetonitrile CH_3CN containing ices have shown an efficient photodesorption pathway of the intact molecule, reaching yields of several 10^{-5} molecules/photons, and which is comparable to the dissociative channels[22,60]. These different trends in the UV photodesorption of organics species may be related to the observations of gaseous organics in the protoplanetary disks: molecules which dissociate efficiently, and whose photodesorption of intact molecules has been experimentally found very low, such as HCOOH or CH_3OH, are very difficult to detect, and observed only in one source[6,61], or even not seen at all in the case of $HCOOCH_3$. On the other hand, acetonitrile, whose intact photodesorption has been observed and measured experimentally, is seen in many sources (e.g. Bergner *et al.* [62]). Such correlation between experimental findings and observation is a strong argument in favor of the key role played by UV photodesorption to explain observed gas phase molecular abundances, including those of organics, in protoplanetary disks and in PDR regions – an hypothesis already formulated in Bergner *et al.* [62] for the CH_3OH and CH_3CN abundances in disks, and in Guzmán *et al.* [5] in the Horsehead nebula. Generalizing the role of UV photodesorption of organics to any cold region of the ISM is however not straightforward, since many other non-thermal desorption processes can be at play, such as chemical desorption or cosmic-ray sputtering of the ices.

4 Conclusions

In this study, we have measured the UV photodesorption yields of neutral species from formic acid HCOOH and methyl formate $HCOOCH_3$ ices – pure and mixed with CO or H_2O – in the 7 – 14 eV range. Our experiments show that the photodesorption process is mostly dominated by the absorption and photodissociation of the solid organics, resulting in the desorption of photofragments or products. Photodesorption yields of H_2O, CO, HCO, H_2CO, and CO_2 were measured from HCOOH-containing ice, and of CH_3, H_2O, CO, HCO, H_2CO, H_3CO, O_2 and CO_2 from $HCOOCH_3$-containing ices. In both cases, the photodesorption yields of the intact HCOOH or $HCOOCH_3$ could not be measured, and only higher limits for the desorption, of 0.5×10^{-5} and 1×10^{-5} ejected molecules per incident photon respectively, could be estimated. The yields are found equal, within our experimental error bars, for pure and mixed ices with CO or H_2O, allowing to propose astrophysical UV photodesorption yields from these two species independent from the ices composition.

To many respects, the UV photodesorption from HCOOH and $HCOOCH_3$-containing ices is similar to UV photodesorption from methanol ices, i.e. a process dominated by the photodissociation of the organics, and in which the desorption of the intact molecule is a minority pathway. This is in contrast to the case of other COMs such as acetonitrile, molecular desorption of which has been shown to compete with its dissociation. This study thus brings new hints that the photodesorption of organics from interstellar ices may actually follow different trends depending on the nature of the considered COM, and that some of them present a methanol-like behaviour, such as HCOOH or $HCOOCH_3$, while other may behave differently.

Many authors tentatively attribute the origin of gas phase HCOOH or $HCOOCH_3$ in the cold media either to the photodesorption (e.g.[5,6]) or to other processes (e.g.[3]), but the lack of quantitative data on the efficiency of each process prevented to actually be able to conclude. In addition, even if the desorption of the intact organics is rather weak as compared to the dissociative channels, the photodesorption of radicals from organics-containing ices is also a potential route to bring reactive material in the gas phase and trigger chemistry leading to the formation of organics. Only a proper astrochemical modelling including the gas-grain exchanges can give a good idea on the relative role played by each processes, which in return implies to know the desorption yields associated with each species. Even if the present study could only provide upper limits to the UV photodesorption of HCOOH and $HCOOCH_3$, it also brings the desorption yields for the desorption of radicals and chemical products from the ices, and it may participate to a better constrain on the role of UV photodesorption as compared to other non-thermal desorption mechanisms in the ISM.

Conflicts of interest

There are no conflicts to declare.

Acknowledgments

This work was funded by (i) the Region Ile-de-France DIM-ACAV+ program, (ii) the Sorbonne Université “Emergence" program, (iii) the ANR PIXyES project, grant ANR-20-CE30-0018 of the French "Agence Nationale de la Recherche" and (iv) the Programme National “Physique et Chimie du Milieu Interstellaire" (PCMI) of CNRS/INSU with INC/INP cofunded by CEA and CNES. We would like to acknowledge SOLEIL for provision of synchrotron radiation facilities under Project Nos. 20191298, and we

gratefully thank L. Nahon for his help on the DESIRS beamline.

Notes and references

1 A. Bacmann, V. Taquet, A. Faure, C. Kahane and C. Ceccarelli, *Astronomy & Astrophysics*, 2012, **541**, L12.

2 I. Jiménez-Serra, A. I. Vasyunin, P. Caselli, N. Marcelino, N. Billot, S. Viti, L. Testi, C. Vastel, B. Lefloch and R. Bachiller, *The Astrophysical Journal*, 2016, **830**, L6.

3 V. Taquet, E. S. Wirström, S. B. Charnley, A. Faure, A. López-Sepulcre and C. M. Persson, *Astronomy & Astrophysics*, 2017, **607**, A20.

4 C. Vastel, C. Ceccarelli, B. Lefloch and R. Bachiller, *The Astrophysical Journal*, 2014, **795**, L2.

5 V. V. Guzmán, J. Pety, P. Gratier, J. R. Goicoechea, M. Gerin, E. Roueff, F. L. Petit and J. L. Bourlot, *Faraday Discuss.*, 2014, **168**, 103–127.

6 C. Favre, D. Fedele, D. Semenov, S. Parfenov, C. Codella, C. Ceccarelli, E. A. Bergin, E. Chapillon, L. Testi, F. Hersant, B. Lefloch, F. Fontani, G. A. Blake, L. I. Cleeves, C. Qi, K. R. Schwarz and V. Taquet, *The Astrophysical Journal Letters*, 2018, **862**, L2.

7 D. Skouteris, N. Balucani, C. Ceccarelli, F. Vazart, C. Puzzarini, V. Barone, C. Codella and B. Lefloch, *The Astrophysical Journal*, 2018, **854**, 135.

8 N. Balucani, C. Ceccarelli and V. Taquet, *Monthly Notices of the Royal Astronomical Society: Letters*, 2015, **449**, L16–L20.

9 A. J. Ocaña, S. Blázquez, D. González, A. Potapov, B. Ballesteros, A. Canosa, M. Antiñolo, J. Albaladejo and E. Jiménez, *Proceedings of the International Astronomical Union*, 2019, **15**, 365–367.

10 D. Qasim, T. Lamberts, J. He, K.-J. Chuang, G. Fedoseev, S. Ioppolo, A. C. A. Boogert and H. Linnartz, *Astronomy & Astrophysics*, 2019, **626**, A118.

11 C. Walsh, E. Herbst, H. Nomura, T. J. Millar and S. W. Weaver, *Faraday Discussions*, 2014, **168**, 389.

12 K. I. Öberg, R. T. Garrod, E. F. van Dishoeck and H. Linnartz, *Astronomy & Astrophysics*, 2009, **504**, 891–U28.

13 A. Ishibashi, H. Hidaka, Y. Oba, A. Kouchi and N. Watanabe, *The Astrophysical Journal Letters*, 2021, **921**, L13.

14 V. Wakelam, E. Dartois, M. Chabot, S. Spezzano, D. Navarro-Almaida, J.-C. Loison and A. Fuente, *Astronomy & Astrophysics*, 2021, **652**, A63.

15 M. Bertin, C. Romanzin, M. Doronin, L. Philippe, P. Jeseck, N. Ligterink, H. Linnartz, X. Michaut and J.-H. Fillion, *The Astrophysical Journal*, 2016, **817**, L12.

16 G. A. Cruz-Diaz, R. Martín-Doménech, G. M. Muñoz Caro and Y.-J. Chen, *Astronomy & Astrophysics*, 2016, **592**, A68.

17 R. Basalgète, R. Dupuy, G. Féraud, C. Romanzin, L. Philippe, X. Michaut, J. Michoud, L. Amiaud, A. Lafosse, J.-H. Fillion and M. Bertin, *Astronomy & Astrophysics*, 2021, **647**, A35.

18 R. Basalgète, R. Dupuy, G. Féraud, C. Romanzin, L. Philippe, X. Michaut, J. Michoud, L. Amiaud, A. Lafosse, J.-H. Fillion and M. Bertin, *Astronomy & Astrophysics*, 2021, **647**, A36.

19 E. Dartois, M. Chabot, T. Barkach, H. Rothard, B. Augé, A. Agnihotri, A. Domaracka and P. Boduch, *Astronomy & Astrophysics*, 2019, **627**, A55.

20 E. Dartois, M. Chabot, A. Bacmann, P. Boduch, A. Domaracka and H. Rothard, *Astronomy & Astrophysics*, 2020, **634**, A103.

21 M. Minissale, F. Dulieu, S. Cazaux and S. Hocuk, *Astronomy & Astrophysics*, 2016, **585**, A24.

22 R. Basalgète, A. J. Ocaña, G. Féraud, C. Romanzin, L. Philippe, X. Michaut, J.-H. Fillion and M. Bertin, *The Astrophysical Journal*, 2021, **922**, 213.

23 K. M. Pontoppidan, H. J. Fraser, E. Dartois, W. F. Thi, E. F. van Dishoeck, A. C. A. Boogert, L. d'Hendecourt, A. Tielens and S. E. Bisschop, *Astronomy & Astrophysics*, 2003, **408**, 981–1007.

24 A. A. Boogert, P. A. Gerakines and D. C. Whittet, *Annual Review of Astronomy and Astrophysics*, 2015, **53**, 541–581.

25 M. Doronin, M. Bertin, X. Michaut, L. Philippe and J.-H. Fillion, *The Journal of Chemical Physics*, 2015, **143**, 084703.

26 M. Bertin, M. Doronin, J.-H. Fillion, X. Michaut, L. Philippe, M. Lattelais, A. Markovits, F. Pauzat, Y. Ellinger and J.-C. Guillemin, *Astronomy & Astrophysics*, 2017, **598**, A18.

27 L. Nahon, N. de Oliveira, G. Garcia, J.-F. Gil, B. Pilette, O. Marcouillé, B. Lagarde and F. Polack, *Journal of Synchrotron Radiation*, 2012, **19**, 508.

28 E. C. Fayolle, M. Bertin, C. Romanzin, X. Michaut, K. I. Öberg, H. Linnartz and J.-H. Fillion, *Astrophysical Journal Letters*, 2011, **739**, L36.

29 . NIST Mass Spectrometry Data Center and E. W. Wallace, in *NIST chemical webbook, NIST standard database n. 69*, ed. P. Linstrom and W. Mallard, National Institute of Standard and Technology, 2022.

30 F. A. Baiocchi, R. C. Wetzel and R. S. Freund, *Physical review letters*, 1984, **53**, 771.

31 K. N. Joshipura, M. Vinodkumar and U. M. Patel, *Journal of Physics B: Atomic, Molecular and Optical Physics*, 2001, **34**, 509.

32 J. R. Vacher, F. Jorand, N. Blin-Simiand and S. Pasquiers, *Chemical Physics Letters*, 2009, **476**, 178–181.

33 R. S. Freund, R. C. Wetzel and R. J. Shul, *Physical Review A*, 1990, **41**, 5861.

34 H. C. Straub, P. Renault, B. G. Lindsay, K. A. Smith and R. F. Stebbings, *Physical Review A*, 1996, **54**, 2146.

35 P. Możejko, *The European Physical Journal Special Topics*, 2007, **144**, 233–237.

36 L. Philippe, T. Hirayama, M. J. Ramage, G. Comtet, M. Rose, L. Hellner and G. Dujardin, *The Journal of Chemical Physics*, 1997, **106**, 7072.

37 M. Bertin, C. Romanzin, X. Michaut, P. Jeseck and J.-H. Fillion, *The Journal of Physical Chemistry C*, 2011, **115**, 12920–12928.

38 C. J. Bennett, T. Hama, Y. S. Kim, M. Kawasaki and R. I. Kaiser, *The Astrophysical Journal*, 2010, **727**, 27.

39 H.-C. Lu, H.-K. Chen, B.-M. Cheng, Y.-P. Kuo and J. F. Ogilvie, *Journal of Physics B: Atomic, Molecular and Optical Physics*, 2005, **38**, 3693–3704.

40 G. A. Cruz-Diaz, G. M. Muñoz Caro, Y.-J. Chen and T.-S. Yih, *Astronomy & Astrophysics*, 2014, **562**, A119.

41 J.-H. Fillion, E. C. Fayolle, X. Michaut, M. Doronin, L. Philippe, J. Rakovsky, C. Romanzin, N. Champion, K. I. Oberg, H. Linnartz and M. Bertin, *Faraday Discussions*, 2014, **168**, 533–552.

42 K. Tabayashi, J.-i. Aoyama, M. Matsui, T. Hino and K. Saito, *The Journal of Chemical Physics*, 1999, **110**, 9547–9554.

43 H. Su, Y. He, F. Kong, W. Fang and R. Liu, *The Journal of Chemical Physics*, 2000, **113**, 1891–1897.

44 M. Hashinokuchi, R. Koumura, D.-C. Che, H. Ohoyama and T. Kasai, *Journal of the Mass Spectrometry Society of Japan*, 2002, **50**, 7–10.

45 M. Schwell, H.-W. Jochims, H. Baumgärtel, F. Dulieu and S. Leach, *Planetary and Space Science*, 2006, **54**, 1073–1085.

46 C.-J. Tso, T. Kasai and K.-C. Lin, *Scientific Reports*, 2020, **10**, 4769.

47 S.-H. Lee, *The Journal of Chemical Physics*, 2008, **129**, 194304.

48 M. Nakamura, P.-Y. Tsai, T. Kasai, K.-C. Lin, F. Palazzetti, A. Lombardi and V. Aquilanti, *Faraday Discussions*, 2015, **177**, 77–98.

49 K. I. Öberg, H. Linnartz, R. Visser and E. F. van Dishoeck, *Astrophysical Journal*, 2009, **693**, 1209–1218.

50 G. A. Cruz-Diaz, R. Martín-Doménech, E. Moreno, G. M. Muñoz Caro and Y.-J. Chen, *Monthly Notices of the Royal Astronomical Society*, 2018, **474**, 3080–3089.

51 J.-H. Fillion, R. Dupuy, G. Féraud, C. Romanzin, L. Philippe, T. Putaud, V. Baglin, R. Cimino, P. Marie-Jeanne, P. Jeseck, X. Michaut and M. Bertin, *ACS Earth and Space Chemistry*, 2022, **6**, 100–115.

52 M. Bulak, D. M. Paardekooper, G. Fedoseev, K.-J. Chuang, J. T. v. Scheltinga, C. Eistrup and H. Linnartz, *Astronomy & Astrophysics*, 2022, **657**, A120.

53 N. G. Petrik, A. G. Kavetsky and G. A. Kimmel, *The Journal of Physical Chemistry B*, 2006, **110**, 2723–2731.

54 J. S. Mathis, P. G. Mezger and N. Panagia, *Astronomy & Astrophysics*, 1983, **128**, 212.

55 R. Gredel, S. Lepp and A. Dalgarno, *the Astrophysical Journal*, 1987, **323**, L137.

56 K. France, E. Schindhelm, E. A. Bergin, E. Roueff and H. Abgrall, *The Astrophysical Journal*, 2014, **784**, 127.

57 R. Dupuy, M. Bertin, G. Féraud, X. Michaut, P. Marie-Jeanne, P. Jeseck, L. Philippe, V. Baglin, R. Cimino, C. Romanzin and J.-H. Fillion, *Physical Review Letters*, 2021, **126**, 156001.

58 M. Bertin, E. C. Fayolle, C. Romanzin, H. A. M. Poderoso, X. Michaut, L. Philippe, P. Jeseck, K. I. Öberg, H. Linnartz and J.-H. Fillion, *The Astrophysical Journal*, 2013, **779**, 120.

59 R. Dupuy, M. Bertin, G. Féraud, X. Michaut, P. Jeseck, M. Doronin, L. Philippe, C. Romanzin and J.-H. Fillion, *Astronomy & Astrophysics*, 2017, **603**, A61.

60 M. Bulak, D. M. Paardekooper, G. Fedoseev and H. Linnartz, *Astronomy & Astrophysics*, 2021, **647**, A82.

61 C. Walsh, R. A. Loomis, K. I. Öberg, M. Kama, M. L. R. v. '. Hoff, T. J. Millar, Yuri Aikawa, E. Herbst, S. L. W. Weaver and H. Nomura, *The Astrophysical Journal Letters*, 2016, **823**, L10.

62 J. B. Bergner, V. G. Guzmán, K. I. Öberg, R. A. Loomis and J. Pegues, *The Astrophysical Journal*, 2018, **857**, 69.